

# Forecasting the spatial extent of the annual flood in the Okavango delta, Botswana

T. Gumbricht<sup>a</sup>, P. Wolski<sup>b</sup>, P. Frost<sup>c</sup>, T.S. McCarthy<sup>a,\*</sup>

<sup>a</sup>*Department of Geology, University of the Witwatersrand, P.O. Box 3, Wits 2050, Johannesburg 4-27125, South Africa*

<sup>b</sup>*Harry Openheimer Okavango Research Centre, University of Botswana, Private Bag 285, Maun, Botswana*

<sup>c</sup>*Institute for Soil, Climate and Water, Private Bag X79, Pretoria 0001, South Africa*

---

## Abstract

The pristine Okavango Delta wetland of northern Botswana is potentially under threat due to water abstraction from its tributaries. We have developed a statistical model which makes it possible to predict the extent of wetland loss which will arise from water abstraction. The model also permits prediction of the maximum area of flooding, and its spatial distribution, three months in advance of the flood maximum. The model was calibrated using maximum areas of seasonal inundation extracted from satellite imagery covering the period 1985–2000, which were correlated with rainfall and total flood discharge. A technique was developed to translate the modelled flood area into a flood map. The methodology can predict maximum area of flooding and its distribution with better than 90% accuracy. An important, although relatively minor, source of error in the spatial distribution of the flood arises from a secular change in flood distribution in the distal Delta which has taken place over the last 15 years. Reconstruction of flooding history back to 1934 suggests that the Delta may be subject to a quasi 80 year climatic oscillation. If this oscillation continues, the extent of flooding will increase in the coming decades.

*Keywords:* Okavango delta; Seasonal flood; Flood forecast; Flood area

---

## 1. Introduction

The Okavango Delta of northern Botswana (Fig. 1) is perhaps the most pristine of Africa's large wetlands, and a major, international tourist destination. Because of its remoteness, it largely escaped colonial development, and its primary sources of water, the Quito and Cubango Rivers, which arise in central Angola and combine to form

the Okavango River, also remain undeveloped. However, in recent years there has been growing interest in the water resources of the region, prompted initially by severe drought conditions in northern Botswana (Scudder, 1993). More recently, a drought in Namibia led to a proposal to pump water from the Okavango River at Rundu as an emergency measure to supply the national water distribution network of that country (Ashton and Manley, 1999). Improved rainfall, however, resulted in temporary suspension of the scheme, but the long term water development plan for

---

\* Corresponding author. Fax: +27-11-717-6579.

E-mail address: mccarthy1@geosciences.wits.ac.za (T.S. McCarthy).

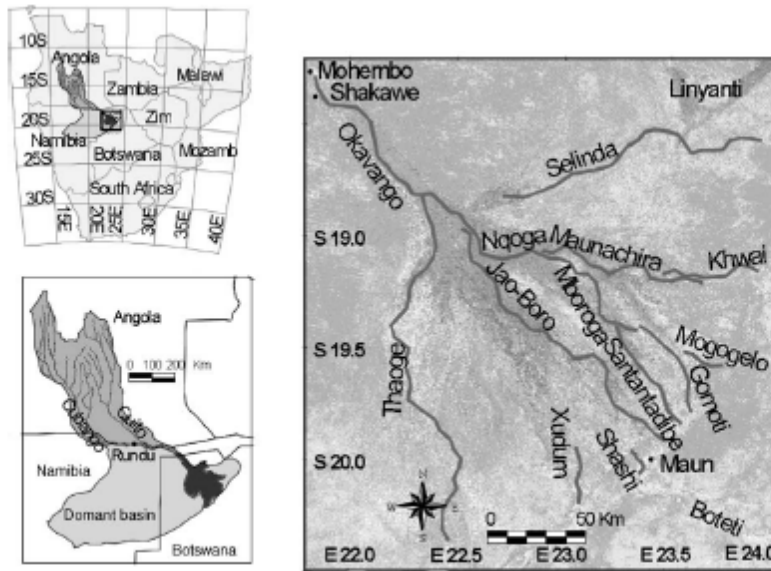


Fig. 1. The Okavango Delta and its catchment.

Namibia involves abstraction of water from the Okavango River (Pallett, 1997). In addition, increasing commercial agriculture along the Okavango River flood plain in Namibia is utilizing progressively more water from the river. Furthermore, the recent end to the long civil war in Angola will result in development of the interior of that country, which will inevitably involve increased water abstraction from the tributaries of the Okavango system.

Water abstraction from the Okavango River and its tributaries poses a threat to the downstream wetland habitats of the Okavango Delta, which depend to a large extent on inflow from the Okavango River, raising the spectre of conflict between development needs and conservation. Attempts have been made in the past to model the effects of water abstraction on the wetlands, but these have examined only the effect on outflow from the wetland (Ashton and Manley, 1999; UNDP, 1976; Dincer et al., 1987; Gieske, 1997). Such outflow is important, because it supplies many rural villages downstream of the Delta, and it

is therefore necessary to understand the impacts water abstraction might have. However, equally important, from a conservation perspective, is the effect abstraction will have on the wetland itself, and in particular on the area of seasonal inundation. Previous models shed minimal light on this subject, because little quantitative data on the area of inundation was available. In this paper we make the first attempt to address quantitatively this extremely important issue.

Local rainfall and inflow to the Delta via the Okavango River have been regularly monitored since the early 1930s, while outflow has been recorded since the early 1970s by government departments in Botswana. We have augmented these data with measurements of the aerial extent of annual flooding extracted from archival satellite imagery extending back to the early 1970s. Using this data base, we have derived a statistical model which can estimate the likely maximum area of the seasonal flood. Images of previous floods of different magnitudes are used to convert the predicted area of inundation into a flood map. The model can be used to investigate the impacts

of water abstraction on the wetland, and can also be used to predict the likely maximum area and spatial extent of flooding in the wetland three months prior to peak flooding.

## 2. Hydrological functioning of the Okavango delta wetland

The Okavango Delta wetland is a large, low gradient (1:3300) alluvial fan, of very low local relief, situated within a depression related to an extension of the East African Rift system (Gumbrecht et al., 2001). Upstream of the fan is an incised corridor known as the Panhandle. The hydrology of the wetland is generally well understood (Wilson and Dincer, 1976; McCarthy et al., 1998). Water is supplied by the Okavango River, whose tributaries, the Quito and Cubango Rivers, rise in the highlands of central Angola. Rain falls in the catchment between December and March, and run-off accumulates in the Okavango River. Peak discharge at the apex of the Panhandle occurs in April. The average annual discharge is  $10.1 \times 10^9 \text{ m}^3$ , but is quite variable, ranging from a low of  $6.0 \times 10^9 \text{ m}^3$  to a high of  $16.4 \times 10^9 \text{ m}^3$  over the last 60 years. The Okavango River meanders down the length of the Panhandle, but at its lower end splits into several distributary channels which direct water to the west (Thaoge), centre (Jao-Boro), and east (Ngoga-Maunachira and Selinda), creating the classic delta shape (Fig. 1). These channels undergo further bifurcation downstream. Channel margins consist mainly of vegetal material and are permeable to water. Consequently, water continually leaks from the channels, and sustains vast backswamp areas. Base flow in the Okavango River sustains about 3000 km<sup>2</sup> of permanent swamp in the Panhandle and around the apex of the alluvial fan, but the area of inundation may seasonally expand and can exceed 12,000 km<sup>2</sup>. Because of the very low gradient, gently undulating topography and dense vegetation, the annual flood wave takes between four and five months to traverse the fan, and maximum inundation on the fan usually occurs in August, in mid-winter.

Whilst the annual inflow from the Okavango River provides an import supply of water, local rainfall also contributes significantly to the wetland. This falls

between October and May, and averages 490 mm/a. Rainfall is derived mainly from convective thunderstorms, is very scattered, and annually very variable. Although the rainfall is moderate, the region is nevertheless semi-arid, with an annual evaporation of 2172 mm, four times annual rainfall. Unusually high rainfall can produce extensive surface flooding during the late summer, well before the normal seasonal flood occurs. These uncommon flood episodes differ from the seasonal flood in that they produce more widespread flooding than the winter seasonal flood, which propagates outward from the apex of the alluvial fan.

The annual flood expands outwards from the fringes of the permanent swamp by a combination of channel and sheet flow. The advancing flood water encounters dry ground, and infiltrates, raising the groundwater table. A considerable proportion of the flood water is thus lost to groundwater recharge. The depth to the groundwater table is therefore an important variable in the overall hydrology of the Okavango Delta. Good summer rains raise the groundwater table, and hence contribute to increasing the area of inundation during the seasonal flood. Antecedent conditions are also important. If the water table is high due to extensive flooding in the previous year, even moderate inflow and rainfall can produce a large area of inundation. The maximum extent of inundation is extremely variable, as is illustrated by two satellite images in Fig. 2a and b. Only about 3% of inflow plus rainfall leaves the Delta via the Boteti River at its southern end, and the bulk of the water is transferred to the atmosphere by evapotranspiration.

## 3. Methodology

### 3.1. Satellite imagery

The spatial extent and area of inundation from 1985 to 2000 was extracted from daily NOAA AVHRR satellite data at 1 km<sup>2</sup> resolution, by using unsupervised classification of geometrically and radiometrically corrected images. The best cloud-free image for each consecutive approximately 10 day period was selected and the area of inundation manually verified. Each image was then compared to the preceding and following images in order to

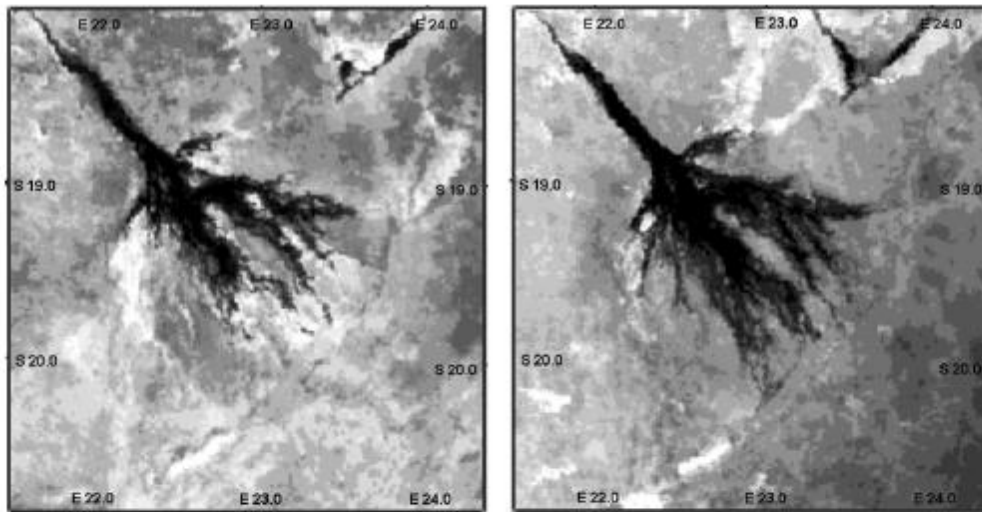


Fig. 2. The area of maximum flood is very variable, as illustrated by the peak floods of 1995 (left) and 2000 (right).

screen for possible erroneous data pixels, and to eliminate the effect of any remaining cloud cover. The areas inundated in the images for each month were aggregated in order to obtain a representative water distribution image for that month. Pixels will be identified as flooded if more than a quarter of the area in that pixel is inundated. For a few dates prior to 1985, LANDSAT TM and MSS data were used as no NOAA data were available. For each image, the area of inundation was extracted. Details of the methodology have been described elsewhere (McCarthy, 2002). The maximum inundated area for each year was determined from the NOAA AVHRR images and these data were used to calibrate the statistical model.

### 3.2. Subdivision of flooded areas

For purposes of analysis, the seasonally inundated region was subdivided into seven sub-regions (Fig. 3). An automatic routine which seeks minimum openness to adjacent areas (Gyllenhammar and Gumbricht, in review) was used to identify these seven sub-regions. The distribution of water in these seven sub-regions at progressively larger areas of total inundation (5000, 6000, 7000 and 8000 km<sup>2</sup>) was extracted in order to investigate secular changes in the distribution of flood water.

### 3.3. Discharge, rainfall and evapotranspiration data

Discharge in the Okavango River and local rainfall are important in determining the area of inundation.

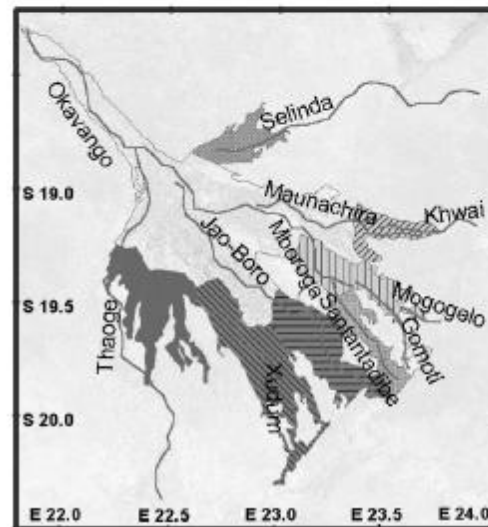


Fig. 3. Sub-regions of the distal portions of the Okavango Delta used to examine secular changes in the distribution of flood water.

Inflow to the Delta has been recorded at Mohebo since 1933, and monthly total discharges were used in this investigation. Rainfall records are available for the villages of Maun from 1921 and Shakawe from 1932. An average of the monthly totals from these two data sets was used as representing local rainfall over the Delta. Rainfall in the region tends to result mainly from local thunderstorms, and is scattered. In order to investigate the possible local influence such scattered showers might have, satellite derived precipitation estimates were obtained for the period 1995–2000 over the entire area (Herman et al., 1997). The variability of rainfall over the seven sub-regions was then examined. Evapotranspiration data were obtained from the weather station at Maun. Records were only available for the period 1967–2000.

#### 3.4. Recreating maps of regions of inundation from a known area of inundation

All images representing the region flooded during the rising flood period were stacked and the sequence of successive filling of the pixels established. This sequence represents the manner in which the flood wave advances. Each pixel is 1 km<sup>2</sup> in area, and hence for any nominated flooded area, a map of the distribution of the water can be constructed by simply filling all the pixels in sequence up to the specified total area. It should be noted that a pixel indicated as flooded may not be entirely inundated, but at least a quarter of that pixel will contain water.

## 4. Results and discussion

### 4.1. Inundation frequency across the Okavango Delta

The Okavango Delta wetland is extremely dynamic, and the area of inundation responds to external variables including the inflow, local rainfall and antecedent effects amongst others. Moreover, the duration of inundation varies spatially, some areas being permanently flooded while other, more distal areas are only flooded infrequently and then for relatively short periods. Rainfall can produce very wide-spread surface flooding. The compiled satellite images of the inundated region provide a means of estimating the percentage time a particular region has

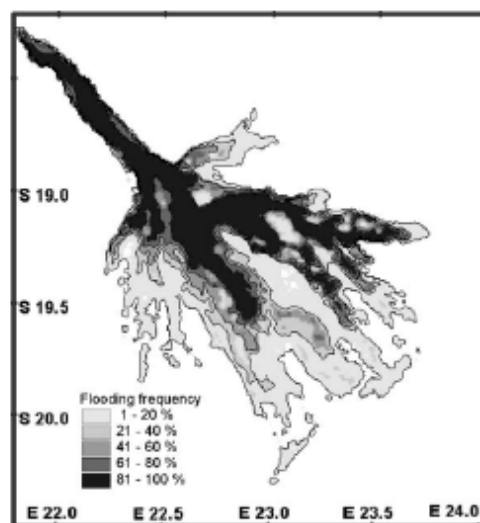


Fig. 4. Map showing the duration of inundation over the period 1985–2000. This diagram includes both the seasonal flooding and inundation due to rainfall.

been inundated over the period 1985–2000 (due to both rainfall and the seasonal flood) and is shown in Fig. 4.

### 4.2. Investigation of secular changes in the distribution of flood water

It has been suggested that there may be long term secular changes in the distribution of flood water in the Okavango Delta. Ellery and McCarthy (Ellery and McCarthy, 1994) reconstructed the probable distribution of flood water over the period from 1850 to the present from historical accounts, and suggest that a major shift has occurred from west along the Thaoge to the east along the Santantidibe-Maunachira system followed by a more recent shift towards the centre (Jao-Boro system) of the Delta.

We investigated whether such shifts were evident in the more limited time period covered by the satellite data series. Fig. 5 shows the distribution of water across the seven sub-regions of the seasonally flooded area (Fig. 3) at progressively increasing area of total inundation, as a function of time. At a total

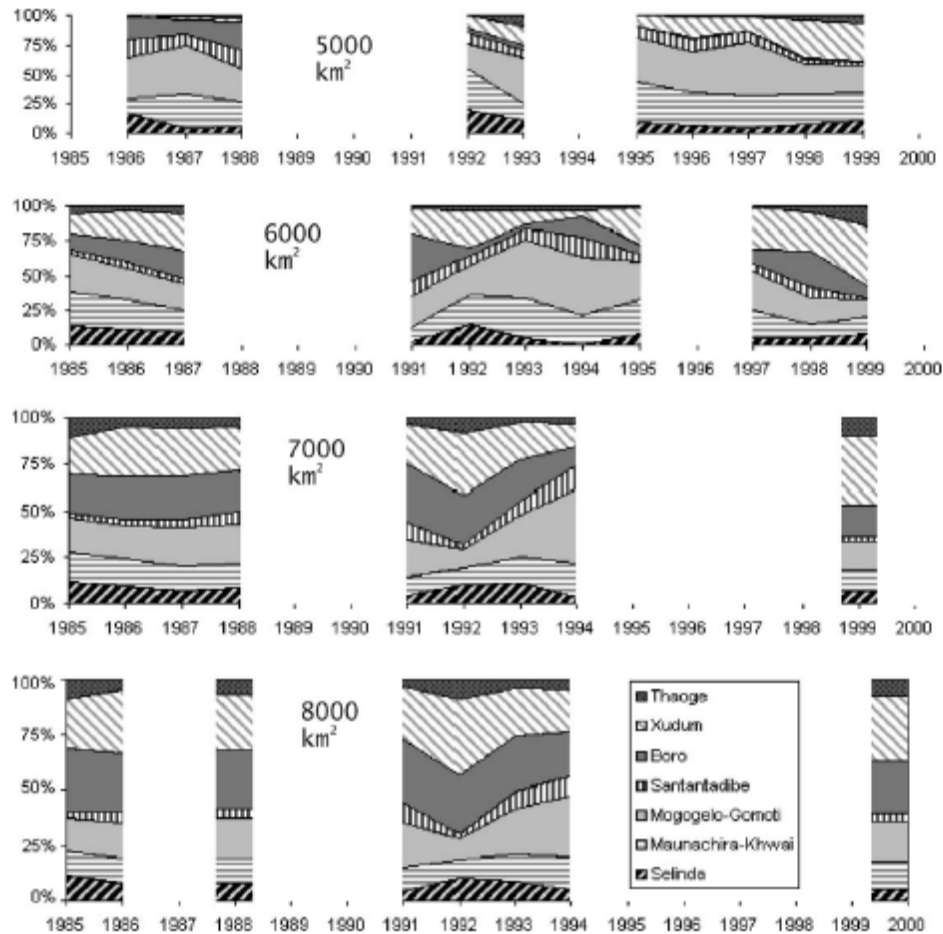


Fig. 5. Distribution of flood waters across the regions shown in Fig. 3 at various stages of the rising flood over the period 1985–2000.

flooded area of  $5000 \text{ km}^2$ , it can be seen that flooding in the Xudum region has grown at the expense of the Boro in the period between 1986 and 1999. However, this increase, although present, is less dramatic at greater areas of inundation. Shift towards the Xudum is more clearly shown in Fig. 6. At low total inundation, the shift is very pronounced, but less so at higher total area of inundation. However, under conditions of very large inflow, as occurred in 1992 and 1999, the Xudum area again appears to receive a larger proportion of water compared to the Boro

(Fig. 5). This shift towards the Xudum system is unlikely to be the result of uneven distribution of rainfall. The distribution of rainfall, based on satellite-derived precipitation estimates, was found to be uniform across the Boro and Xudum areas in the period 1995–2000, and this situation probably also obtained in previous years.

There does therefore appear to be a progressive shift towards the Xudum at the expense of the Boro, which at intermediate levels of inundation tends to be somewhat masked. This shift may be the explanation

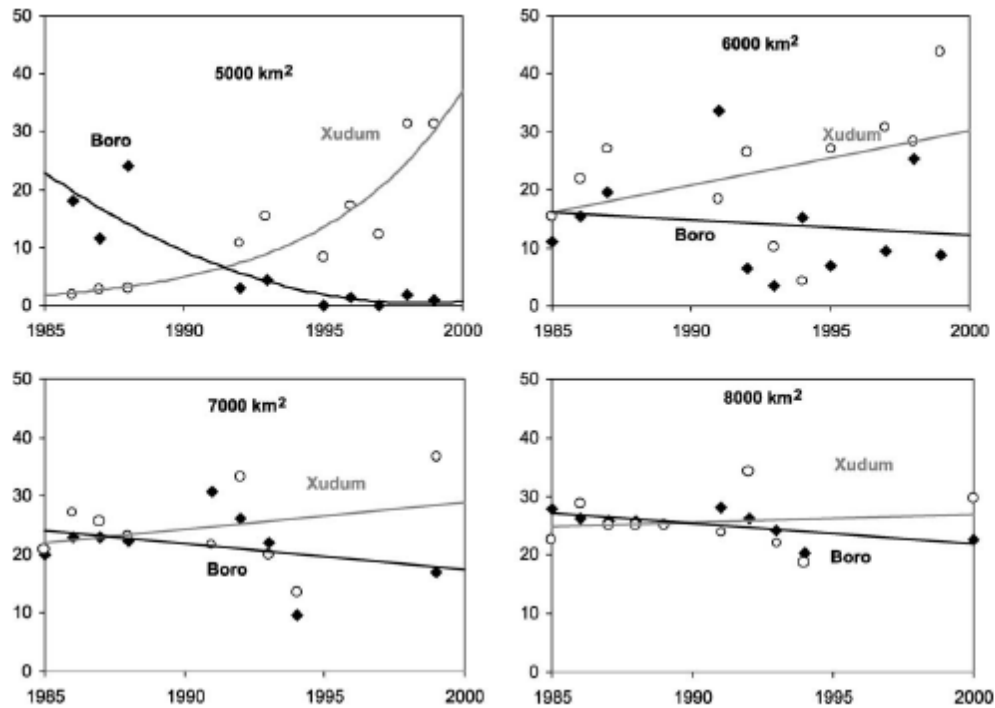


Fig. 6. Changes in the distribution of water in the Xudum and Boro distributary systems over time (horizontal axis) at different flooding stages, expressed as a percentage (vertical axis) of the total discharge to the seven sub-regions of the distal portion of the Okavango shown in Fig. 3.

for the decreasing discharges in the Shashi River over the last two decades, which have caused a decline in the recharge of the well field along this river, and in turn have resulted in water shortages in Maun.

The cause of the shift from the Boro to the Xudum regions is uncertain, and two possible mechanisms may be at work, either separately or in concert. McCarthy et al. (1997) detected a tectonic disturbance at the upper end of the Boro region as defined in Fig. 3, which has created a southwesterly orientated graben structure across the Boro channel, and has also induced local incision of the channel. This tectonic disturbance may possibly be diverting flood water towards the southwest into the Xudum region. Diversion of water may also be under the influence of dense aquatic vegetation in the upper Boro region, which may have a more pronounced effect at low inundations, but less at high inundation when the flood stage is higher.

Fig. 5 also confirms previous observations (McCarthy et al., 1998; Gumbricht et al., 2000) that the major seasonal flood is accommodated in the region to the west of Chief's Island, mainly by the Boro and Xudum systems, which show the greatest proportional increase as the total area of inundation rises. Although it is evident from the regional topography that the Selinda region is the most relatively depressed portion of the Delta (Gumbricht et al., 2001), and hence should receive substantial flood water, the area of flooding along the Selinda actually declines proportionally at large total flooding. This suggests that entry of water into the Selinda region is being severely restricted near its head. Discharge into the Nqoga channel system which flows to the east is similarly restricted, which reduces the area of seasonal swamp in the eastern portion of the Delta (McCarthy et al., 1998).

#### 4.3. Statistical model of the area of inundation

It has been previously shown that the most important variables in determining the magnitude of seasonal flooding are seasonal inflow and total summer rainfall (Gieske, 1997; McCarthy et al., 1998). In addition, second order effects arise from evapotranspirational loss of water and groundwater recharge. Rainfall, inflow and evapotranspiration data exist for the period covered by the satellite data, but the amount of water lost to groundwater recharge cannot be determined. However, a proxy measure is provided by the extent of flooding in the preceding year. Maximum flooding in the Delta generally occurs in August, in response to inflow which peaks in April, and rainfall which peaks in February. For the purposes of the statistical analysis, therefore, the total discharge measured at Mohebo between November of the preceding year and August (i.e. the seasonal flood wave) and the rainfall in the same period were compared with the maximum area of flooding, extracted from the satellite data. The maximum area of flooding in the preceding year was used to represent the antecedent effect. Multiple regression was performed, with maximum area of inundation serving as the dependant variable. The regression yielded the following equation:

$$A(\text{km}^2) = 0.79 \times Q(10^6 \text{m}^3) + 5.59 \times P(\text{mm}) + 0.059 \times L(\text{km}^2) - 817 \quad (1)$$

where  $A$  is the maximum inundated area,  $Q$  the inflow,  $P$  the rainfall and  $L$  the area of flooding in the preceding year. The correlation between calculated and actual area of inundation yielded an  $R^2$  of 0.90, with a standard error of 589  $\text{km}^2$ . Including evapotranspiration in the analysis yielded the following equation:

$$A(\text{km}^2) = 0.79 \times Q(10^6 \text{m}^3) + 5.33 \times P(\text{mm}) + 0.084 \times L(\text{km}^2) - 442 \times E(\text{mm}) + 1386 \quad (2)$$

where  $E$  is the measured evapotranspiration. The correlation between calculated and actual inundated areas yielded an  $R^2$  of 0.90, with a standard error of 613  $\text{km}^2$ .

While a model based on inflow from November to August is realistic in terms of including the entire

flood wave, it has a disadvantage in that it provides no predictive capability. Peak discharge usually occurs in April, and falls thereafter. The earliest date at which the impact of seasonal inflow can begin to be assessed is therefore the end of May. A model incorporating inflow in this period could provide a predictive capability on the extent of the impending seasonal flood. Accordingly statistical models based on this shorter time period were investigated. Regression analysis using inflow and rainfall between November and May yielded the following equation:

$$A(\text{km}^2) = 0.94 \times Q(10^6 \text{m}^3) + 6.03 \times P(\text{mm}) + 0.107 \times L(\text{km}^2) - 901 \quad (3)$$

Correlation between calculated and actual inundated areas yielded an  $R^2$  of 0.87 and a standard error of 667  $\text{km}^2$ .

Including evapotranspirational loss in the regression yielded the following equation:

$$A(\text{km}^2) = 0.96 \times Q(10^6 \text{m}^3) + 5.59 \times P(\text{mm}) + 0.148 \times L(\text{km}^2) - 747 \times E(\text{mm}) + 2811 \quad (4)$$

Correlation between predicted and actual inundated areas yielded an  $R^2$  of 0.87 and a standard error of 695  $\text{km}^2$ .

It is evident from the above analysis that adding evapotranspiration provided no improvement. The probable reason for this is that evapotranspiration varies very little from year to year. There is a slight loss of accuracy introduced by reducing the period of inflow (standard error rises from 585  $\text{km}^2$  using Eq. (1) to 667  $\text{km}^2$  using Eq. (3)), but this is more than compensated for by the predictive capability resulting from the statistical model based on the shorter time period. Modelled results (using Eq. (3)) are compared with actual flooded areas over the investigation period in Fig. 7.

#### 4.4. Reconstructing maps showing the inundated region from calculated total area of inundation

The statistical model described above can predict the area of inundation fairly well, with an error margin of less than 10% (mean area of maximum inundation of the period used in the analysis was 7666  $\text{km}^2$ ),



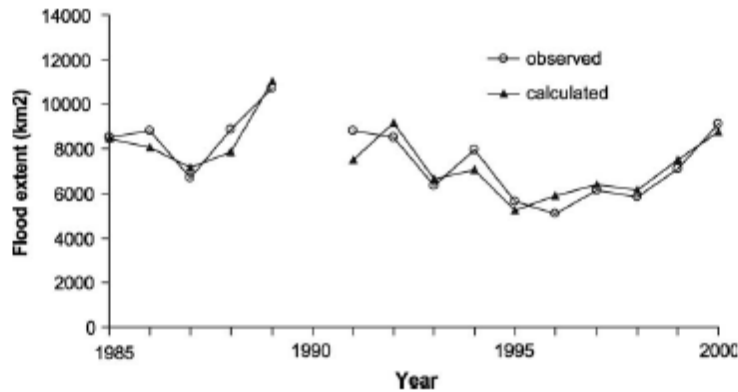


Fig. 7. A comparison of the actual area of inundation with that modelled using Eq. (3) over the period 1985–2000.

and hence can be used to model the effects of water abstraction from the Okavango River. Knowing the area of wetland likely to be lost as a result of water abstraction is useful, but equally useful would be information on where the loss will occur. In order to obtain this information, it is necessary to be able to translate a modelled total area of inundation into a map showing flood distribution. The satellite derived maps of flood extent described above (see Section 3) were developed for this purpose. Fig. 8 shows eight of these maps at progressively increasing area of total inundation. Fig. 9 shows a comparison of an actual flooded area (Fig. 9a) with one reconstructed from the general model for a year with abnormally high rainfall (2000), and Fig. 10 for a year with abnormally low rainfall (1995). Figs. 9b and 10b show the estimated areas of flooding with plus and minus one standard error for the two respective years. The actual areas of inundation are shown by the solid line. The actual area of flooding generally falls within the limits set by one standard error interval, except in the Xudum area, where flooding has increased over time, and is hence underestimated in the model-derived flood maps.

As discussed above, there appears to be a slow secular switch in flood distribution from the Boro to the Xudum system which will alter the distribution of flood water in the future. The maps shown in Fig. 8 therefore will have a limited currency, and will probably need to be updated in the future. The discrepancies are larger for low total inundation, and

the maps will be valid for a longer period if used for high total inundation.

The Namibian national water plan calls for the abstraction of 120 million m<sup>3</sup> per annum from the Okavango River at Rundu (P. Heyns, pers. comm. to TSM, although reported by Pallett (1997), to be 100 million m<sup>3</sup>). The statistical model indicates that this will result in the loss of 114 km<sup>2</sup> of wetland (the model is linear, and 95 km<sup>2</sup> of wetland will be lost per 100 million m<sup>3</sup> of water abstracted per annum). Spatial reconstruction indicates that the loss will be very widely distributed along the shoreline of the wetland (Fig. 11). In reality, the real loss is likely to be even more widely spread than indicated by the model, because the spatial resolution of the model is 1 km<sup>2</sup>, which tends to shorten the shoreline.

The model defined by Eq. (3) uses inflow from November to May and rainfall over the same period, and therefore can be used to predict the maximum extent of flooding (in August), some three months ahead of the peak. An ability to predict the extent of flooding in advance could be useful to tour, air charter and logistical support companies operating in the Delta, although local calibration may be necessary, as the resolution of the model is fairly coarse. This local calibration would involve assessing in what way a particular flood level will affect, for example, road access to safari lodges and availability of air fields, based on past experience.

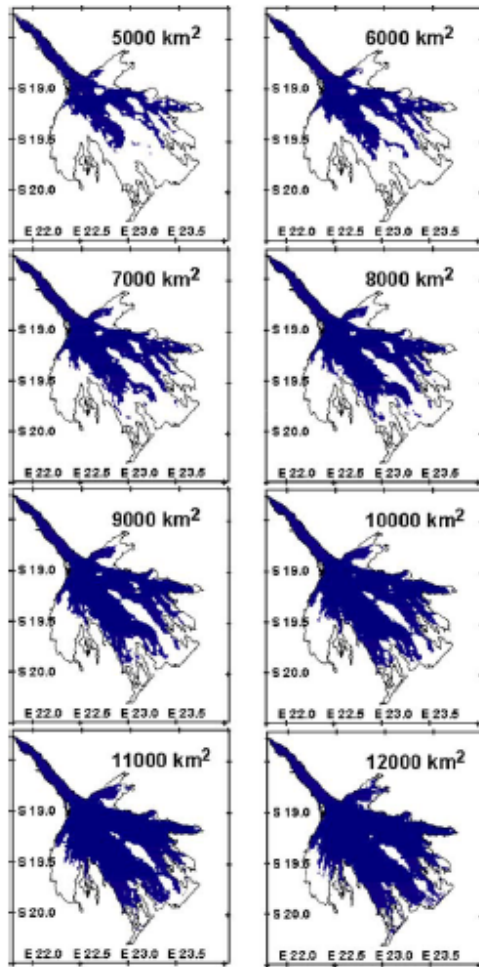


Fig. 8. Maps showing the extent of flooding at increasing areas of total inundation. The outline indicates the maximum likely flood as indicated by vegetation patterns and satellite images.

#### 4.5. The relationship between annual outflow from the Delta and the maximum area of inundation

The relationship between maximum area of inundation (modelled using Eq. (1)) and measured outflow for the year (from February to January) is

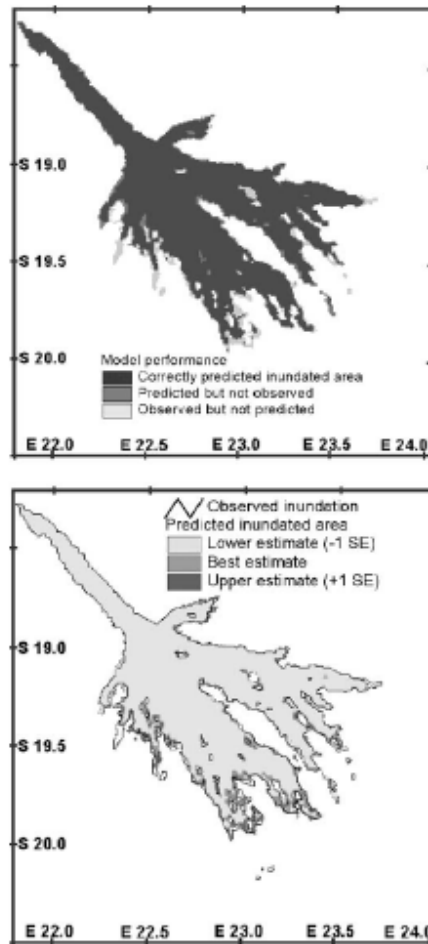


Fig. 9. A comparison of the actual area of inundation (top) with that reconstructed from the model using Eq. (3) for a year with above average rainfall (2000); bottom diagram shows the estimated area of flooding for 2000 with plus and minus one standard error interval. The solid line demarcates the actual maximum flood in that year.

shown in Fig. 12. With increasing inundation, outflow rises at a progressively higher rate. This suggests that at greater extents of inundation, there is less impedance to flow from vegetation and less loss to groundwater recharge, and hence progressively greater outflows result.

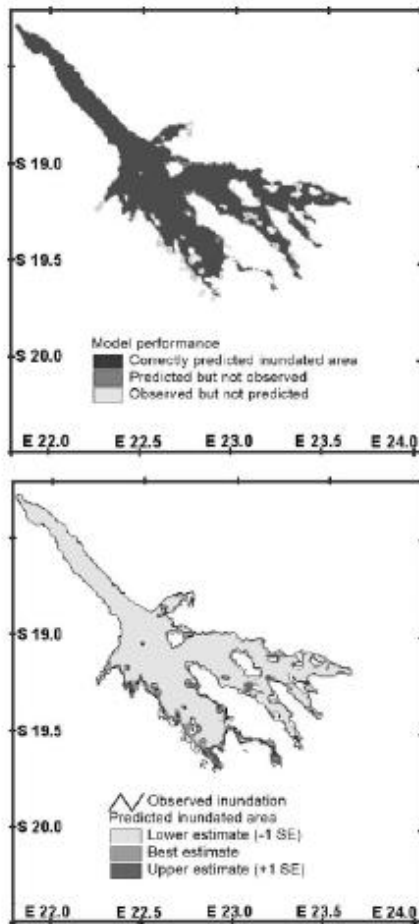


Fig. 10. A comparison of the actual area of inundation (top) with that reconstructed from the model using Eq. (3) for a year with low average rainfall (1995); bottom diagram shows the estimated area of flooding for 1995 with plus and minus one standard error interval. The solid line demarcates the actual maximum flood in that year.

#### 4.6. Long term changes in maximum area of inundation

The statistical model described above makes it possible to estimate past areas of inundation. These have been reconstructed back to 1934 using Eq. (1), when local rainfall records and Okavango River

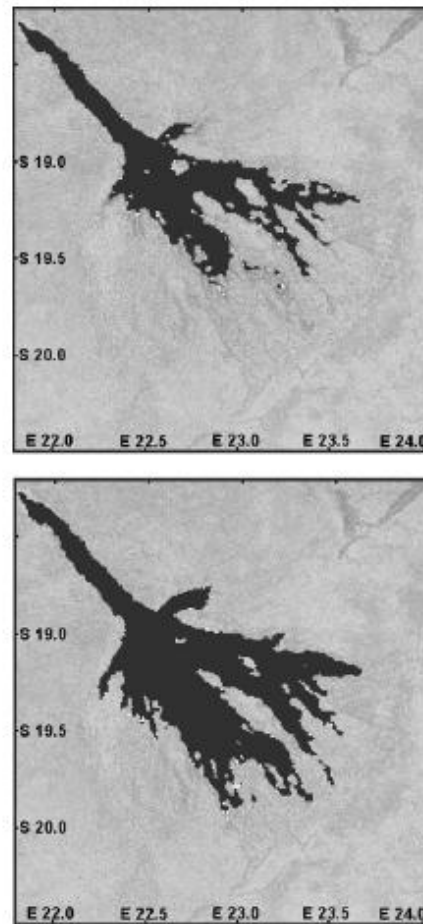


Fig. 11. Maps showing the wetland areas expected to be lost (in white) as a result of the abstraction of 120 million  $m^3$  of water per annum from the Okavango River, for the years 1995 (top) and 2000 (bottom).

discharges first became simultaneously available. An arbitrary flood was assumed for 1933 to provide the initial antecedent component term in the statistical model. Thereafter, the calculated value was used over the entire period. The results of the calculations are shown in the form of total area in Fig. 13a and as a deviation from the long term average (9970  $km^2$ ) in

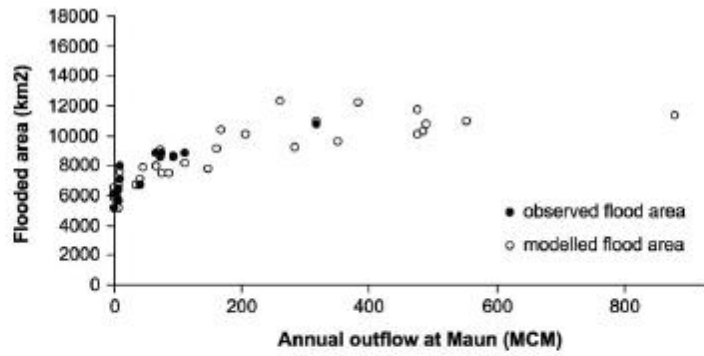


Fig. 12. The relationship between area of inundation (modelled using Eq. (3) and determined using the NOAA AVHRR images) and measured annual outflow from the Delta.

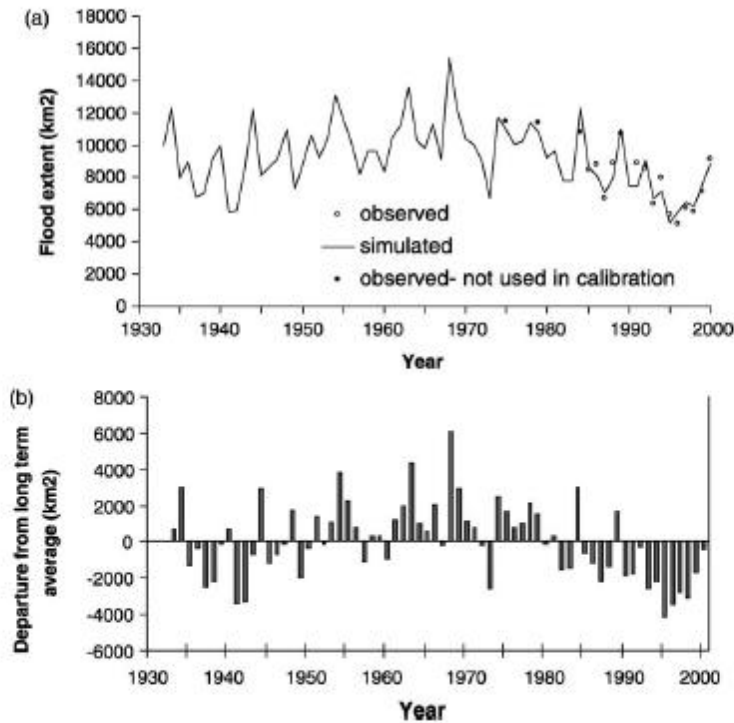


Fig. 13. (a) Modelled annual maximum flood for the period 1934–2000. The circles represent flooded areas measured from satellite images. The 1985–2000 measured areas (open circles) were used in calibrating the model. (b) Modelled annual maximum flood expressed as a deviation from the long term average for the period 1934–2000.

Fig. 13b. In Fig. 13a, the actual flooded areas for the period 1985–2000 are included for comparison, together with some earlier years for which data are available. It is evident from this figure that the flooded area calculated using the internally generated antecedent flood predict actual flood reasonably accurately (mean annual error is 564 km<sup>2</sup>).

These diagrams, especially Fig. 13b, suggest a long term oscillation in the area of inundation. Prior to about 1950 and after 1980, flooded area was generally below the long term average, while above average floods characterized the period from about 1950–1980. This pattern is strikingly similar to that seen in measured discharges in the Zambezi River (McCarthy et al., 2000).

The hydrology of the Okavango Delta results from a complex interplay between local rainfall and discharges in the two tributaries of the Okavango River, the Quito and Cubango Rivers. An analysis of past records of these three components was recently undertaken by McCarthy et al. (2000), which showed that the discharge records for the Quito River and the rainfall over the Delta were generally above the long term average in the period 1950–1980, while the Cubango River showed no clear pattern. The general trend evident for the Delta as a whole suggests that in the combination of the three components, the records of the Quito and local rainfall together strongly influence the pattern for the Delta as a whole. McCarthy et al. (2002) suggest that the pattern evident in the flooding of the Delta and in the Zambezi discharge arises from a quasi 80 year climatic oscillation.

## 5. Conclusions

Archival NOAA AVHRR and LANDSAT data have made it possible to obtain information on the aerial extent and spatial distribution of seasonal floods in the Okavango Delta wetland over the past three decades. The maximum inundated area extracted from these satellite data together with local rainfall and annual discharge in the Okavango River have been used to produce a model which can predict the area of flooding with a high degree of confidence. This statistical model makes it possible, for the first time, to assess quantitatively the effect that water abstraction from the Okavango River will have on the Okavango wetland. Calculations indicate that 95 km<sup>2</sup> of wetland will be lost for every 100 million m<sup>3</sup> per annum of

water abstracted from the river. The model can also be used to predict the maximum area of flooding some three months in advance, which could be useful to companies operating in the area.

The statistical model is useful, but it is also essential to know where the loss will occur, if wetland is to be lost. Information extracted from the satellite data allows the reconstruction of the spatial distribution of flooding from a calculated total flooded area. It is therefore possible not only to predict the extent of a flood but also its spatial distribution, and this can be used to determine where loss of wetland will occur if abstraction of water takes place, and in addition, to investigate this under conditions of varying total area of inundation.

The satellite records indicate that the most extensive seasonal flooding occurs to the west of Chief's Island, and moreover the data show that a gradual shift in water distribution in this region has taken place over the last two decades. The Boro channel has lost water to the Xudum system to the east, and may be the cause of the failing recharge of the well field on the Shashi River, which supplies Maun.

Flooding history over the last 70 years shows that during the period 1950–1980, the area inundated was significantly greater than the long term average, a feature also shown by the discharge in the Zambezi River. The Delta, like the Zambezi, may be under the influence of a quasi 80 year climatic oscillation. The implication of this observation is that there will be a steady rise in maximum inundated area over the next few decades. This, coupled with the shift in water distribution from the Boro towards the Xudum, is likely to result in the refilling of Lake Ngami. However, there are negative consequences for safari and aircraft operators in that certain access roads and air fields in the Delta are likely become unuseable for several months of the year if flood conditions return to the high floods of the 1950–1980 period.

## Acknowledgements

The Department of Water Affairs and the MET Office of the Government of Botswana are thanked for supplying data for this study. Jenny McCarthy and Frank Siedel are thanked for assistance with data processing. Funding was provided by Swedish International Development Agency,

the National Research Foundation of South Africa, and the Universities of the Witwatersrand and Botswana.

## References

- Ashton, P., Manley, R., 1999. Potential hydrological implications of water abstraction from the Okavango River in Namibia. Ninth South African Hydrological Symposium, South Africa, November, 1–10.
- Dincer, T., Child, S., Khupe, B., 1987. A simple mathematical model of a complex hydrological system: Okavango swamp, Botswana. *Journal of Hydrology* 93, 41–65.
- Ellery, W.N., McCarthy, T.S., 1994. Principles of sustainable utilization of the Okavango Delta ecosystem, Botswana. *Biological Conservation* 70, 159–168.
- Gieske, A., 1997. Modelling outflow from the Jao/Boro system in the Okavango Delta, Botswana. *Journal of Hydrology* 193, 214–239.
- Gumbrecht, T., McCarthy, J., McCarthy, T.S., 2000. Portraying the geophysiology of the Okavango Delta, Botswana. 28th International Conference on Remote Sensing of the Environment. Cape Town, South Africa. CD ROM publication.
- Gumbrecht, T., McCarthy, T.S., Merry, C.L., 2001. The topography of the Okavango Delta, Botswana, and its sedimentological and tectonic implications. *South African Journal of Geology* 104, 243–264.
- Herman, A., Kumar, V.B., Arkin, P.A., Kousky, J.V., 1997. Objectively determined 10-day African rainfall estimates created for famine early warning systems. *International Journal of Remote Sensing*, 18(10): 2147–2159.
- Herman, A., Kumar, V.B., Arkin, P.A., Kousky, J.V., 1997. Objectively determined ten-day African rainfall estimates created for famine early warning systems. <http://edcintl.cr.usgs.gov/adda>.
- McCarthy, J., 2002. Remote sensing for detection of landscape form and function of the Okavango Delta. PhD Thesis TRITA-LWR. PHD 1000, Department of Land and Water Resources Engineering, Royal Institute of Technology, Stockholm, Sweden, 50pp.
- McCarthy, T.S., Barry, M., Bloem, A., Ellery, W.N., Heister, H., Merry, C.L., Ruther, H., Sternberg, H., 1997. The gradient of the Okavango Fan Botswana, and its sedimentological and tectonic implications. *Journal of African Earth Sciences* 24, 65–78.
- McCarthy, T.S., Larkin, P.A., Bloem, A., 1998. Observations on the hydrology and geohydrology of the Okavango Delta. *South African Journal of Geology*, 101–117.
- McCarthy, T.S., Cooper, G.R.J., Tyson, P.D., Ellery, W.N., 2000. Seasonal flooding in the Okavango Delta Botswana—recent history and future prospects. *South African Journal of Science* 96, 25–33.
- Pallett, J., 1997. *Sharing Water in Southern Africa*, Desert Research Foundation of Namibia, Windhoek, Namibia, pp. 121.
- Scudder, T., 1993. The IUCN review of the Southern Okavango Integrated Water Development Project. IUCN, Gland, Switzerland, pp. 541.
- UNDP, 1976. Investigation of the Okavango as a primary water resource for Botswana. Technical Report, United Nations Development Programme/Food and Agricultural Organization. BOT/71/506. 3 volumes.
- Wilson, B.H., Dincer, T., 1976. An introduction to the hydrology and hydrography of the Okavango Delta, Proceedings of a Symposium on the Okavango Delta, Botswana Society, Gaborone, Botswana, pp. 33–48.